Hindawi
International Journal of Polymer Science
Volume 2019, Article ID 9123635, 9 pages
https://doi.org/10.1155/2019/9123635

Research Article

Effects of Zinc-Free Processing Aids on Silica-Reinforced Tread Compounds for Green Tires

Nam Chul Kim and Sung Ho Song

Division of Advanced Materials Engineering, Kongju National University, Chungnam 32588, Republic of Korea

Correspondence should be addressed to Sung Ho Song; shsong805@gmail.com

Received 13 December 2018; Revised 18 January 2019; Accepted 30 April 2019; Published 25 June 2019

Academic Editor: Mehdi Salami-Kalajahi

With the development of "green tires" in the tire industry, the conventional carbon black filler that is used in tread formulations is being replaced with silica. Generally, this requires the addition of a processing aid, containing zinc ion, which acts as a lubricant and dispersing agent. However, because zinc is a heavy metal, zinc-free processing aids (ZFAs) are required to satisfy worldwide environmental concerns. We present herein a series of catalytically synthesized ZFAs and evaluate the effects of replacing zinc ion-containing processing aids (ZCAs) on a silica tread formulation. Interestingly, replacing ZCA with ZFA in a two parts per hundred rubber (phr) by weight formulation improved both its tensile strength and elongation by as much as 31% and 20%, respectively. ZFA-rubber formulations also exhibited a twofold enhancement in fatigue properties over those of ZCA-rubber formulations. Furthermore, pneumatic tires were fabricated from our ZFA-rubber formulation and compared against tires containing ZCAs. The ZFA-rubber composite exhibited improved dry and wet braking and rolling resistance due to enhanced dispersion of silica in the rubber matrix. These results show that rubber composites prepared with ZFAs may be promising in tire engineering applications.

1. Introduction

Carbon black is an important filler that enhances the physical and mechanical properties, including tear strength, hardness, and abrasion resistance, of almost all industrial rubbers [1–3]. In recent years, however, "green tires" made with silica fillers instead of carbon black have exhibited greater abrasion resistance and wet grip, as well as lower rolling resistance [4–6]. Silica, which bears silanol and siloxane functional groups, differs from carbon black in both chemical composition and method of manufacture [7]. Silanol groups are acidic [8] and interact with basic accelerators, thereby slowing cure rates and lowering the cross-link density in sulfur-cured systems [9]. The viscosity of a formulation increases with the amount of silica particles, which tend to interact strongly with themselves due to their polar and hydrophilic nature [10]. Thus, silica-containing formulations are more difficult to process, and silica particles are relatively difficult to disperse in a rubber matrix [11–14]. Silane coupling agents have been used to modify the surface of silica particles to enhance rubber-filler interactions. These include TESPT (bis(triethoxysilylpropyl)tetrasulfide) and TESPD (bis(triethoxysilylpropyl)disulfide), which, due to their bifunctional characteristics, act as chemical bonding agents between the rubber matrix and silica during vulcanization [15–17].

The processing agents used in the manufacture of tire rubbers are classified according to their chemical structure and include hydrocarbons, low molecular weight polymers, fatty acid derivatives, synthetic resins, and other organic compounds. Several additives, such as fatty acid esters, act as lubricants and/or dispersion agents. In particular, bifunctional silanes containing sulfur have been used to improve processability during mixing and the chemical bonding between silica and rubber. Currently, zinc soaps such as zinc stearate, zinc naphthenate, and zinc resinate are used as processing agents in rubber formulations. Most zinc soaps act as intermolecular lubricants because they are rubber-soluble. However, zinc consumption is a worldwide environmental concern, and the automotive industry, as a main

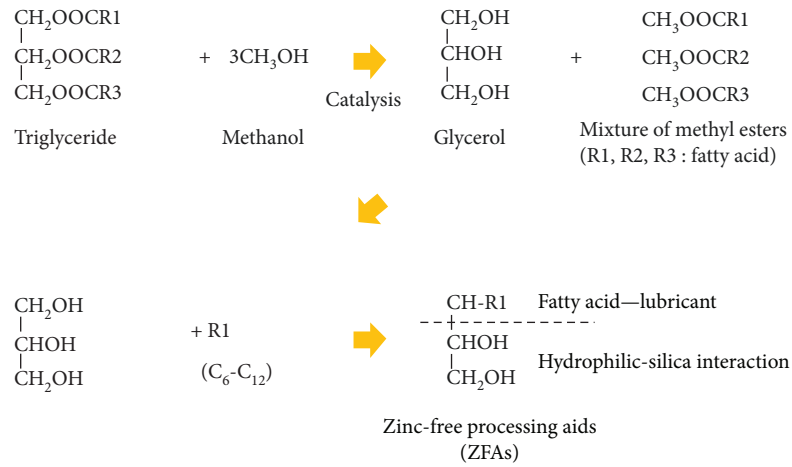

Figure 1: A schematic diagram showing the preparation of zinc-free processing aids (ZFAs).

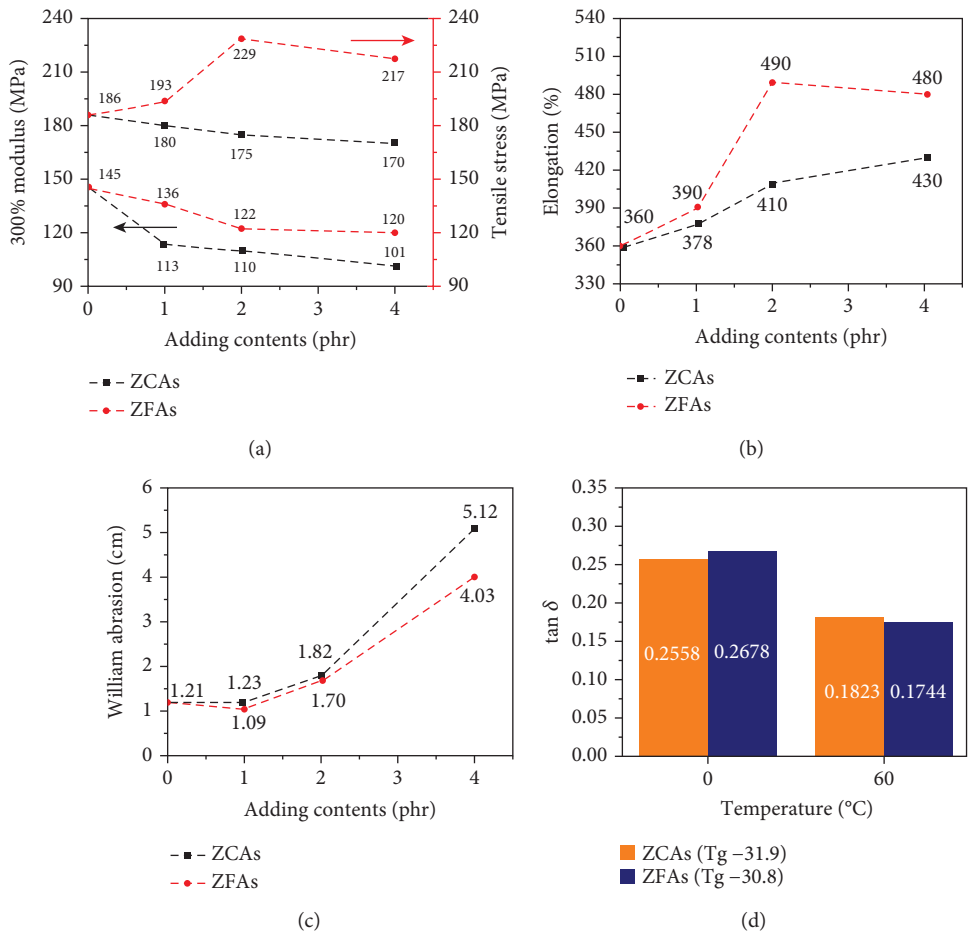

Figure 2: (a) Modulus and tensile strength, (b) elongation, (c) William abrasion, and (d) dynamic properties (tan δ) of rubber composites with zinc ion-containing processing aids (ZCAs) and ZFAs.

contributor, is under increasing pressure to decrease its share. Although large amounts of zinc-containing additives are used in the automotive industry, there are relatively few studies that address zinc-free processing aids (ZFAs).

The current study describes the catalytic fabrication of ZFAs having hydrophilic groups and fatty acid at opposite ends of the molecule. This structure serves to enhance the dispersion of silica in the rubber matrix. The fatty acid group

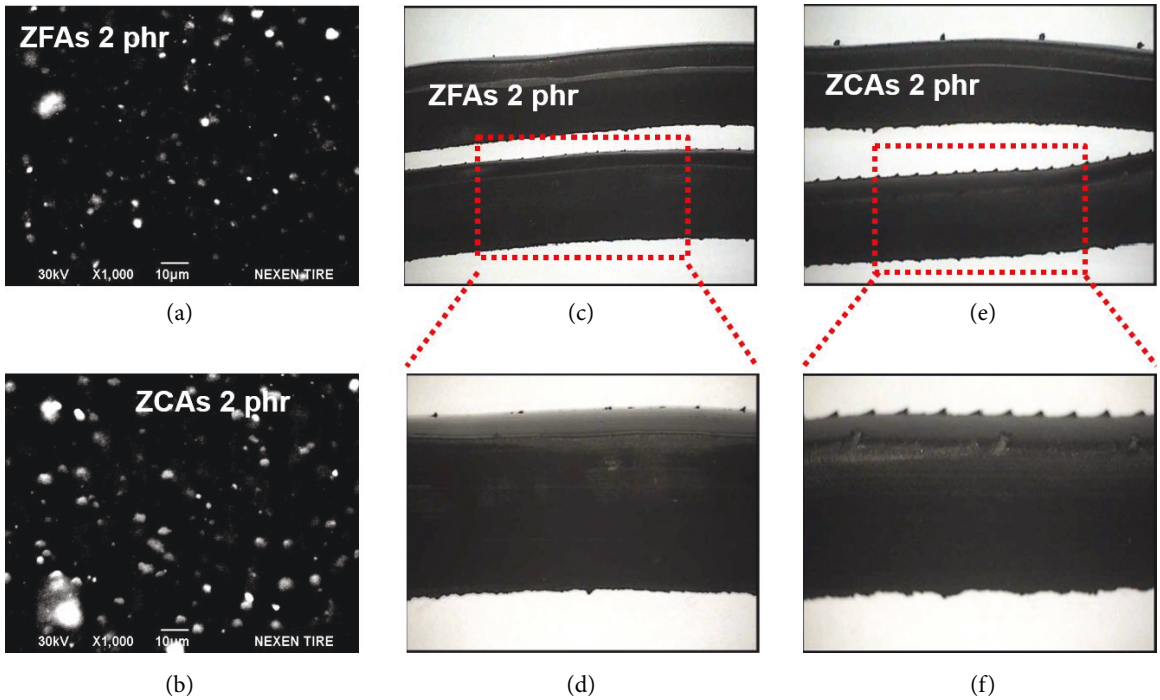

Figure 3: Scanning electron microscopy (SEM) micrograph of rubber composites made with (a) ZFAs and (b) ZCAs. (c) Images of Garvey die extrusions of rubber composites made with (c) ZFAs (enlarged image in (d)) and (e) ZCAs (enlarged image in (f)).

reacts with double bonds on the rubber chain [18, 19], while the hydrophilic group reacts with silanols on the silica surface [20, 21]. This report also evaluates the effects of conventional and silica-based processing aids in styrene butadiene rubber (SBR) during mixing and after vulcanization. A master batch of SBR, made with typical processing aids and a silica filler, was used to improve their dispersion in a rubber latex matrix through a latex mixing method. This method was a scalable, versatile, inexpensive, fast, and convenient method of enhancing the performance of rubber composites. Silica rubbers containing ZFAs exhibited more desirable mechanical, fatigue, and abrasion properties than those of zinc ion-containing processing aids (ZCAs). Furthermore, ZFAs were added to the SBR tread compound used to manufacture a pneumatic tire to represent the possibility of "green tires" containing the silica fillers. This tire boasted a low rolling resistance and highly improved grip in both dry and wet conditions. This research shows the advantages and potential of silica-based fillers for tire engineering.

2. Experimental Section

2.1. Materials. An SBR (SBR 1500) consisting of 23% styrene and 77% butadiene was purchased from Kumho Petrochemical Co. Ltd., Korea. The silica and coupling agent used in this study were supplied by Solvay. Silicas and zinc ion processing aids were obtained from Struktol Co., USA. Also, carbon black (N 330) was obtained from OCI Co. Ltd., Korea, and N-*tert*-butyl-benzothiazole sulfonamide (TBBS) were purchased from Shangdong Shanxian Co. Ltd., China. Zinc oxide (ZnO), stearic acid (S/A), and sulfur were purchased from Sigma-Aldrich.

2.2. Preparation of ZFAs. Glycerol was formed through the catalytic reaction of triglycerides, KOH, and NaOH in methanol. The molar ratio of glycerol and fatty acid is 2 : 1 and mixed with a metal catalyst until the acid value was zero at 400 rpm at 200°C for 5 h in an inert atmosphere.

2.3. Preparation of Rubber Composites. SBR/silica composites with processing aids were fabricated by the standard processes in Tables S2 and S3. In Table S2, firstly, an SBR latex (20 phr (parts per hundred rubber) by weight) containing 20 phr silica with ZFAs and ZCAs was mixed by vigorous stirring for 24 h. An SBR latex (20 phr) was also prepared with silica (20, 40, and 60 phr) and contained ZFAs and ZCAs at 2 phr in Table S3. This mixture was also mixed for 24 h. The processing aids/silica-SBR composites were then coagulated with a sulfuric acid solution (1.0 phr). The composites were rinsed with water until the pH of the rinsate was 6~7 and then dried in an oven at 50°C for 24 h. Then, SBR (80 phr) and silica (20 phr)/SBR (20 phr) latex and various additives in a Banbury mixer at a rotor speed of 60 rpm were mixed. Finally, to initiate the curing process, the vulcanization agents and additives were added at the end of mixing. The fabrication process of the SBR composites is presented in Tables S2 and S3.

2.4. Characterization. Scanning electron microscopy (SEM; JEOL JSM-6490LV) was used to observe the morphology of fractured surfaces of rubber composites. The moving die

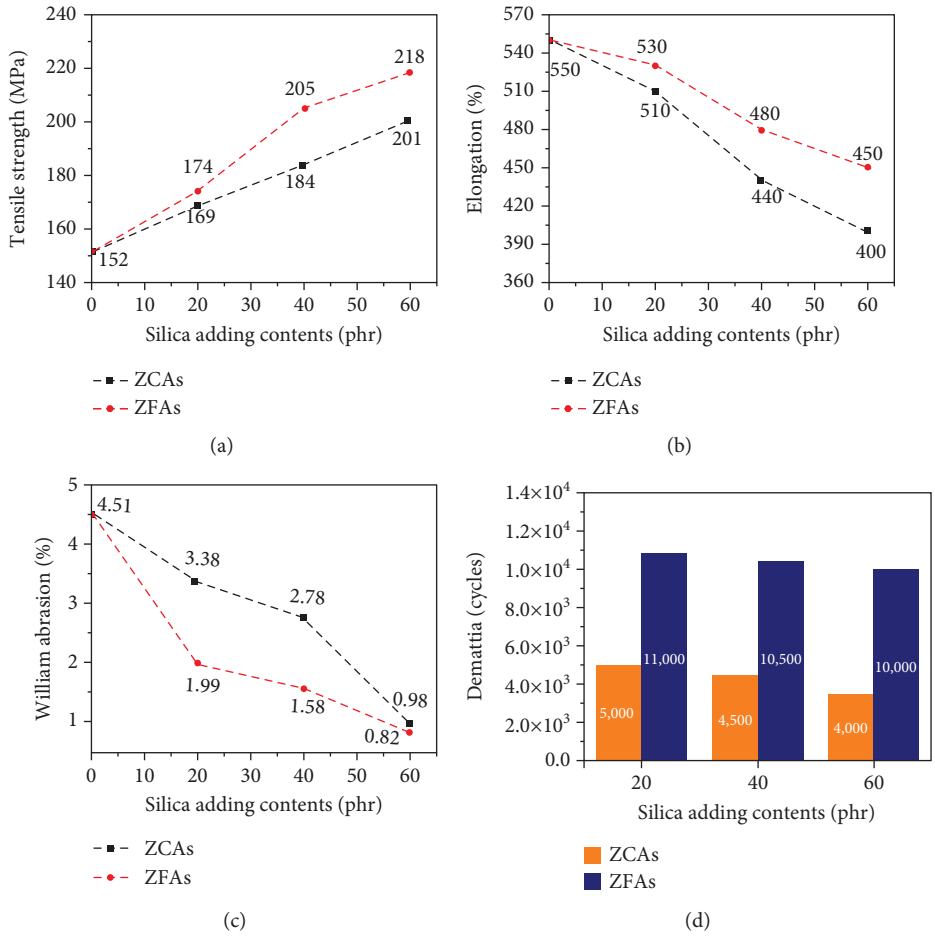

Figure 4: (a) Tensile strength, (b) elongation, (c) William abrasion, and (d) fatigue properties (fatigue crack generation) of rubber composites containing ZCAs or ZFAs with varying degrees of silica loading.

rheometer test (MCR 702; Anton Paar) was observed to analyze the cure properties of the resulting materials under pressure. Mechanical tests (modulus, tensile strength, and elongation) were conducted with dumbbell-shaped samples (length: 100 mm, width: 5 mm) by using an Instron tensile machine (Instron Co., UK) at a speed of 300 mm/min. At least four tests were conducted for each type of sample. Dynamic properties were carried out in a tensile mode in a dynamic mechanical analyzer (DMA 50N01Db-METRAVIB). Also, the tan delta (temperature sweep of the loss factor) and the storage modulus were measured from 20°C to 120°C (heating rate: 3°C/min, frequency: 10 Hz).

3. Characterization of Results and Discussions

We present a series of ZFAs fabricated by the catalytic reaction shown in Figure 1. Figure 1 presents the preparation of glycerol using triglycerides and a metal catalyst in methanol through catalytic reaction. This process afforded ZFAs bearing both hydrophilic and hydrophobic groups in large quantities. Due to the absence of zinc in the former, the melting points of the ZFAs were lower than those of the corresponding ZCAs, as shown in Table S1. The ZFAs were pelletized so that they were more easily incorporated into tire engineering applications. The properties of ZFAs are confirmed by the spectroscopic analysis and thermogravimetric analysis (TGA) in Figure S1. The chemical structure of the ZFAs was analyzed by X-ray photoelectron spectroscopy (XPS). The C1s signal consisted of three different peaks: the C-C bond (284.5 eV), C-O (286.6 eV), and C=O (288.2 eV) of the carbonyl groups in Figure S1a. Also, the peaks of O1s and C=O peaks (530.5 eV and 532.8 eV) were showed in the ZFAs from the O1s scan (Figure S1c). In the FT-IR spectra, ZFAs are shown C-H stretching and C-OH stretching peaks in carbonyl and carboxylic acid groups in Figure S1d. Furthermore, in the TGA result, mass of ZFAs begins to lose at 100°C and completely decomposes at 400°C.

Figures 2(a) and 2(b) show a comparison of the modulus, tensile strength, and elongation of SBR composites as a function of increasing ZFA or ZCA content. Modulus and tensile strength decreased with increasing amounts of processing aid, while elongation increased due to increasing viscosity. The modulus and tensile strength of composites containing ZFAs (2 phr) were as much as 11% and 31% greater than those containing ZCAs, respectively. This

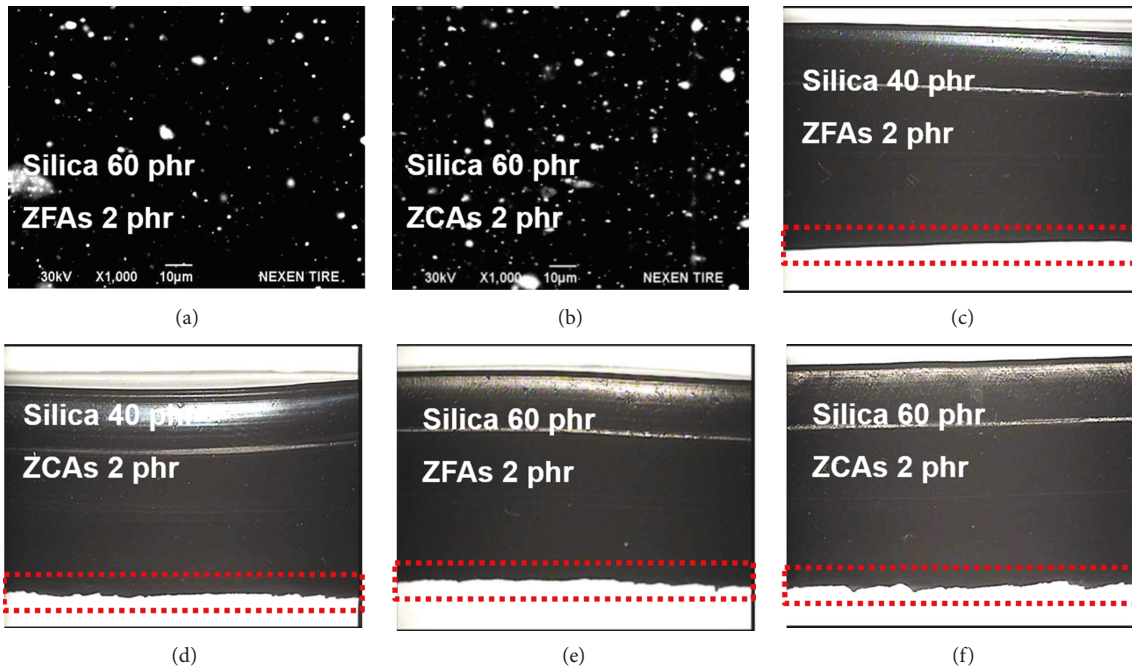

Figure 5: SEM micrographs of (a) ZFA- and (b) ZCA-rubber composites with 60 parts per hundred rubber (phr) silica. Garvey die extrusion images of (c) ZFA (2 phr)- and (d) ZCA (2 phr)-rubber composites with 40 phr silica and (e) ZFA (2 phr)- and (f) ZCA (2 phr)-rubber composites with 60 phr silica.

performance enhancement was due to the amphoteric nature of ZFAs and the resulting stronger interfacial bonding and improved dispersion of silica within the elastomer matrix and the restriction of segmental elastomer chain motion. Figure 2(b) shows that the elongation at break of ZFA/SBR composites (490%) was greater than that of ZCA composites (410%). The increased reinforcement can be attributed to the large contact area between silica and the elastomer matrix. Figure 2(c) shows the abrasion properties of SBR composites containing ZFAs or ZCAs. The amount of abrasion loss, on the whole, increased with the amount of processing aid due to the increasing viscosity of the composites. Note that the ZFA/SBR composites exhibited greater wear resistance (William wear 4.03%) due to enhanced silica dispersion and cross-linking density. The dynamic mechanical properties (DMA), such as tan δ (the ratio of loss modulus to storage modulus), of SBR composites containing ZFAs and ZCAs are shown as a function of temperature in Figure 2(d). DMA tests can be used to predict both wet traction and rolling resistance [22]. With the addition of ZFAs, the tan δ of 0°C was about 5% higher than that of SBR composites containing ZCAs. This implies that pneumatic tires incorporating ZFAs have the potential for improved wet grip tire performance. Furthermore, the 60°C tan δ of the ZFA/SBR composites was about 5% lower than that of the ZCA/SBR composites, indicating a potentially lower rolling resistance of the former [23, 24].

The physical properties of SBR composites with ZFCs and containing other processing aids were studied. The constrained region (rubber chains immobilized on the surface of fillers) serves as a commercializer in rubber composites. This reinforcement is enhanced by the filler and prevents phase separation, and the weight fraction of rubber chains immobilized on the surface of fillers (χ_m) can be calculated as follows:

$$\Delta C_{pn} = \frac{\Delta C_p}{(1-\omega)},$$
$$\chi_{im} = \frac{(\Delta C_{p0} - \Delta C_{pn})}{\Delta C_{p0}}, \quad (1)$$

where ΔC_p is the heat capacity jump at the glass transition temperature (T_g), ΔC_{pn} is the heat capacity jump normalized to the rubber fraction, ΔC_{p0} represents the heat capacity jump at the T_g of the neat rubber, and ω is the weight fraction of fillers in the composites. Also, the heat capacity changes were measured by differential scanning calorimetry (DSC). In Table S4, the value of χ_{im} for ZFCs/SBR is much higher than those of the ZCAs/SBR compositions.

The SEM micrographs in Figures 3(a) and 3(b) and S1 show that silica (20 phr) disperses evenly throughout ZFA/SBR composites without coagulation. Figure S2 also shows that increasing the proportion of ZFA decreased the number of coagulated particles in the rubber matrix. This result supports the Garvey Die Extrusion tests. A Garvey die in a Haake torque rheometer was used to monitor the sheet forming and extrusion behavior of the SBR composites. Figures 3(c)–3(f) show extrusion quality as a function of the type of processing aid. Figures 3(c) and 3(d) and S3 show that rubber extrusions containing a high

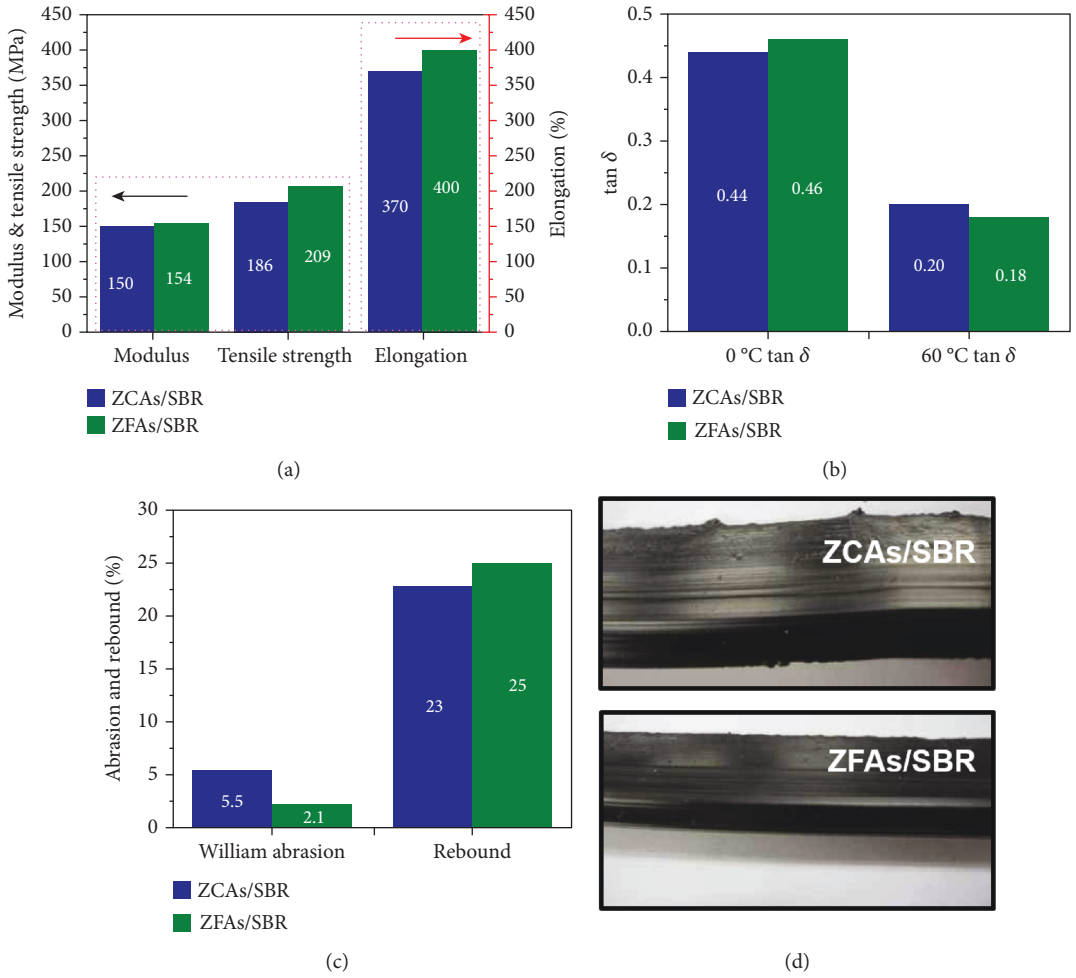

Figure 6: (a) Modulus, tensile strength, and elongation, (b) dynamic properties (tan δ), (c) abrasion and rebound, and (d) Garvey die extrusion images of tire tread compounds made with ZCA/styrene butadiene rubber (SBR) or ZFA/SBR composite.

loading of ZFA exhibited smoother and more stable edges. This effect was likely due to the relatively high viscosity of the ZFA formulations. Figures 3(e) and 3(f) show that extrusions made with the ZCA/SBR composites had rougher surfaces and more unstable edges.

Tensile strength and elongation of SBR composites are shown as a function of silica loading in Figures 4(a) and 4(b). While the addition of silica resulted in significant increases in tensile strength (Figure 4(a)), it also resulted in decreased elongation (Figure 4(b)). Compared to ZCA/SBR composites, the tensile strength and elongation of ZFA/SBR composites containing 60 phr silica increased to 218 MPa and 450%, corresponding to enhancements of 8% and 12.5%, respectively, while the modulus remained unchanged (Figure S4). Figure 4(c) shows that abrasion resistance also increased with increasing silica content. The William abrasion test of ZFA-rubber composites was lower than that of ZCA composites, implying improved dispersion of silica in the rubber matrix. The fatigue properties of SBR composites with various processing aids are shown in Figure 4(d). In general, reductions in fatigue life were observed with increasing silica content. However, the fatigue life of ZFA/SBR composites was more than twice that of ZCA/SBR composites. This is likely due to the more uniform dispersion of ZFAs in the rubber matrix.

SEM micrographs of silica (60 phr)/SBR composites containing 2 phr of processing aids show that the silica was evenly dispersed in the ZFA/SBR composites without coagulation (Figures 5(a) and 5(b) and S5). Furthermore, Figure S4 shows that both the degree of dispersion and the uniformity of distribution of silica were enhanced with the use of ZFAs. This result is also supported by the fatigue properties of silica treads shown in Figure S5. After 10,000 cycles, the crack length in silica treads made with ZFA/SBR composite was approximately 26% greater than that of treads made with ZCA/SBR. Figures 5(c)–5(f) show that ZFA (2 phr)/SBR composites yielded smoother extrusions with more stable edges compared to those made with ZCA/SBR composites.

Pneumatic tires were made with each composite to confirm the superior performance of the ZFA/SBR composites. The results of mechanical tests are given in Figure 6. Figure 6(a) compares the physical properties of SBR composites made with different processing aids. The modulus and tensile strength of tread compounds made with ZFA/SBR were as much as 3% and 12% greater than those of the

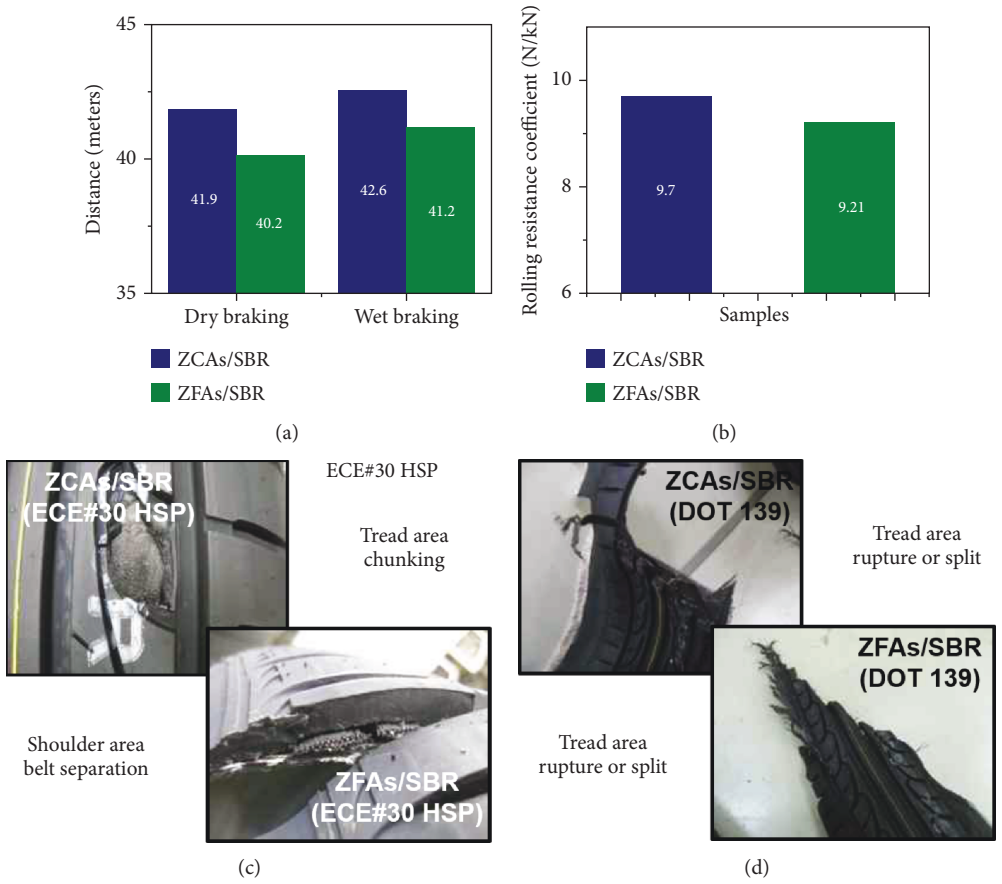

Figure 7: (a) Dry and wet braking properties, (b) rolling resistance coefficients, (c) high-speed durability (ECE#30 HSP), and (d) high-speed durability (DOT 139) of pneumatic tires made with ZCA/SBR or ZFAs/SBR composite.

control, respectively. In addition, the elongation of ZFA/SBR treads was significantly greater than that of ZCA/SBR treads. The elongation of ZFA/SBR treads increased by 8%. As discussed above, this enhancement is attributed to strong interfacial bonding and improved dispersion of silica within the rubber matrix.

The DMA of a particular rubber formulation is important because rubber composites are frequently subjected to dynamic loading. Figure 6(b) shows the DMA of pneumatic tires, including tan δ of the control and ZFA/SBR composite tires, as a function of temperature. While the tan δ of 0°C for ZFA/SBR treads was about 5% higher than that of the control, the tan δ of 60°C was about 11% lower than that of the control. These data demonstrate the potential of pneumatic tires with ZFAs for enhanced rolling resistance and wet grip [23, 24]. The abrasion and rebound properties of silica tread compounds are shown in Figure 6(c). The William abrasion test of pneumatic tires made with ZFAs was more than two orders of magnitude higher than that of the control. This is attributed to rubber-filler interactions among ZFA particles. The effect of ZFA loading on rebound resilience at room temperatures is given in Figure 6(c). The percent rebound resilience of ZFA/SBR composites was about 9% greater than that of ZCA/SBR composites. This result indicates that the presence of ZFAs improves the elasticity of rubber composites due to increased cross-link density between silica and the rubber matrix. This agrees with the results of Garvey die extrusion tests shown in Figure 6(d). Due to the higher viscosity of the ZFA formulations, extrusions made with ZFA/SBR composites exhibited stable edges and a smoother shape than those made with the control composite.

Finally, virtual tests were performed using a vehicle-mounted pneumatic tire made with ZFA/SBR or ZCA/SBR composite rubbers. The results are shown in Figure 7. Generally, the high-speed durability and rolling resistance of the tires play important roles in characteristics of vehicle dynamics [25, 26]. The data in Figures 7(a) and 7(b) show that treads made with ZFA/SBR composites exhibited lower rolling resistance with increased grip under braking in both wet and dry conditions. The pneumatic tire with ZFA/SBR compounds shows dry and wet braking properties improved by 4% and 3% compared to the control compound, respectively. Also, in Figure 7(b), the pneumatic tire with the ZFA/SBR compound (9.21 N/kN) exhibits an improved rolling resistance coefficient compared to the control compound (9.7 N/kN). These results are due to the improved viscoelastic properties by strong interfacial interactions between silica and the rubber matrix in ZFA/SBR composites. Finally, Figures 7(c) and 7(d) show the results of high-speed endurance tests of the ECE (Economic Commission for Europe) #30 HSP and DOT (US Department of Transportation)

139. The DOT guidelines ensure that a tire meets or exceeds the safety requirements of the US Department of Transportation, and ECE#30 is a European guideline that sets requirements for tire size, rolling resistance, braking, and high-speed durability. In general, tire failure occurs in belt separation due to the heat generated by external impact and movement in high-speed tests. In Figure 7(c), though the pneumatic tire with the ZCA/SBR compound generated chunks due to reduced durability, belt separation occurs in the pneumatic tires with the ZFA/SBR compound. Furthermore, similar results were obtained in DOT tests in Figure 7(d). The closer the silica filler aggregates to each other, the greater the desorption and heat concentration, which means that polymer chains can more easily break away from the silica particles, resulting in a drop in mechanical properties [27, 28].

4. Conclusion

ZFAs were synthesized using a catalytic reaction and evaluated in rubber compositions used for tire treads. The incorporation of ZFAs into SBR rubber matrices resulted in remarkable improvements in modulus, tensile strength, elongation, and dynamic properties. These enhancements were attributed to uniform dispersion of silica particles, and enhanced interfacial bonding between these particles and the SBR, in the rubber matrix. This study also demonstrates the ease with which ZFA/SBR composites can be integrated into a rubber matrix using a new, versatile, and simple approach based on latex technology. Furthermore, ZFA/SBR composites were employed directly as additives in the tread of a pneumatic tire. Tires fabricated with the ZFA/SBR composite exhibited significantly improved dry and wet braking, rolling resistance, and high-speed durability due to enhanced dispersion of silica in the compounds. These results also demonstrate the effectiveness of ZFA processing aids in the production of elastomer composites for use at low loading levels.

Data Availability

The data used to support the findings of this study are available from the corresponding author upon request.

Conflicts of Interest

The authors declare that there are no conflicts of interest regarding the publication of this paper.

Authors' Contributions

S.H.S. provided guidance in performing the research, and N.C.K. performed FT-IR, XPS, and TGA experiment of the rubber composites and analyzed the data. All authors were involved in extensive discussion and data analysis.

Acknowledgments

The research was supported by the International Science and Business Belt Program through the Ministry of Science and ICT (2017K000488). Also, this research was supported by the research grant of the Kongju National University in 2015.

Supplementary Materials

Table S1: characteristics of the ZFAs. Table S2: formation of rubber composites with varying loading fraction of processing aids. Table S3: formation of rubber composites with varying loading fraction of silica. Table S4: the parameter values of SBR composites with varying loading fraction of processing aids. Figure S1: characterization of as-prepared ZFAs. Figure S2: SEM images of rubber composites with varying loading fraction of ZFAs and ZCAs. Figure S3: Garvey Die Extrusion images of rubber composites with varying loading fraction of ZFAs. Figure S4: modulus of rubber composites with ZCAs and ZFAs with varying loading fraction of silica. Figure S5: SEM images of rubber composites with ZCAs and ZFAs with varying loading fraction of silica. Figure S6: fatigue properties of rubber composites with ZCAs and ZFAs. *(Supplementary Materials)*

References

[1] S. H. Song, "Synergistic effect of carbon nanofiber decorated with iron oxide in enhancing properties of styrene butadiene rubber nanocomposites," *Journal of Applied Polymer Science*, vol. 134, no. 40, pp. 45376–45384, 2017.

[2] S. H. Song, "Synergistic effect of clay platelets and carbon nanotubes in styrene–butadiene rubber nanocomposites," *Macromolecular Chemistry and Physics*, vol. 217, no. 23, pp. 2617–2625, 2016.

[3] S. P. Lee, O. S. Kwon, Y. G. Kang, and S. H. Song, "Styrene butadiene rubber/clay nanocomposites for tire tread application," *Plastics, Rubber and Composites*, vol. 45, no. 9, pp. 382–388, 2016.

[4] L. Zhang, S. Wen, Y. Lu, H. Yang, and J. Shen, "Surface modification of silica by two-step method and properties of solution styrene butadiene rubber (SSBR) nanocomposites filled with modified silica," *Composites Science and Technology*, vol. 88, no. 14, pp. 69–75, 2013.

[5] Y. Lin, P. Liu, J. Peng, and L. Liu, "The filler–rubber interface and reinforcement in styrene butadiene rubber composites with graphene/silica hybrids: a quantitative correlation with the constrained region," *Composites Part A: Applied Science and Manufacturing*, vol. 86, pp. 19–30, 2016.

[6] K. Kim, J.-Y. Lee, B.-J. Choi et al., "Styrene-butadiene-glycidyl methacrylate terpolymer/silica composites: dispersion of silica particles and dynamic mechanical properties," *Composite Interfaces*, vol. 21, no. 8, pp. 685–702, 2014.

[7] M. A. Ansarifar, T. Nanapoolsin, and A. Jain, "Silane-silica reinforcement of some natural rubber vulcanisates," *Journal of Rubber Research*, vol. 5, no. 2, pp. 11–27, 2002.

[8] S. Wolff, U. Görl, M. J. Wang, and W. Wolff, "Silane modified silicas-silica-based tread compounds," *European Rubber Journal*, vol. 16, no. 1, pp. 16–19, 1994.

[9] A. Ansarifar, L. Wang, R. J. Ellis, and S. P. Kirtley, "The reinforcement and crosslinking of styrene butadiene rubber with silanized precipitated silica nanofiller," *Rubber Chemistry and Technology*, vol. 79, no. 1, pp. 39–54, 2006.

[10] A. Ansarifar, L. Wang, R. J. Ellis, S. P. Kirtley, and N. Riyazuddin, "Enhancing the mechanical properties of

styrene–butadiene rubber by optimizing the chemical bonding between silanized silica nanofiller and the rubber," *Journal of Applied Polymer Science*, vol. 105, no. 2, pp. 322–332, 2007.

[11] K. J. Kim and J. VanderKooi, "Effects of zinc ion containing surfactant on bifunctional silane treated silica compounds in natural rubber," *Journal of Industrial and Engineering Chemistry*, vol. 8, no. 4, pp. 334–347, 2002.

[12] K. J. Kim and J. L. White, "Silica agglomerate breakdown in three-stage mix including a continuous ultrasonic extruder," *Journal of Industrial and Engineering Chemistry*, vol. 6, no. 6, pp. 372–379, 2000.

[13] N. G. Eskandar, S. Simovic, and C. A. Prestidge, "Interactions of hydrophilic silica nanoparticles and classical surfactants at non-polar oil–water interface," *Journal of Colloid and Interface Science*, vol. 358, no. 1, pp. 217–225, 2011.

[14] S. Simovic and C. A. Prestidge, "Hydrophilic silica nanoparticles at the PDMS droplet–water interface," *Langmuir*, vol. 19, no. 9, pp. 3785–3792, 2003.

[15] F. Vilmin, I. Bottero, A. Travert et al., "Reactivity of bis[3-(triethoxysilyl)propyl] tetrasulfide (TESPT) silane coupling agent over hydrated silica: operando IR spectroscopy and chemometrics study," *Journal of Physical Chemistry C*, vol. 118, no. 9, pp. 4056–4071, 2014.

[16] L. Qu, G. Yu, X. Xie, L. Wang, J. Li, and Q. Zhao, "Effect of silane coupling agent on filler and rubber interaction of silica reinforced solution styrene butadiene rubber," *Polymer Composites*, vol. 34, no. 10, pp. 1575–1582, 2013.

[17] F. Yatsuyanagi, N. Suzuki, M. Ito, and H. Kaidou, "Effects of surface chemistry of silica particles on the mechanical properties of silica filled styrene–butadiene rubber systems," *Polymer Journal*, vol. 34, no. 5, pp. 332–339, 2002.

[18] C. J. Brinker, "Hydrolysis and condensation of silicates: effects on structure," *Journal of Non-Crystalline Solids*, vol. 100, no. 1-3, pp. 31–50, 1998.

[19] B. K. Coltrain and L. W. Kelts, "The chemistry of hydrolysis and condensation of silica sol—gel precursors," *Advances in Chemistry*, vol. 234, 418 pages, 1994.

[20] E. C. de Oliveira Nassor, L. R. Ávila, P. F. dos Santos Pereira, K. J. Ciuffi, P. S. Calefi, and E. J. Nassar, "Influence of the hydrolysis and condensation time on the preparation of hybrid materials," *Materials Research*, vol. 14, no. 1, pp. 1–6, 2011.

[21] J. G. Seo, C. K. Lee, D. Lee, and S. H. Song, "High-performance tires based on graphene coated with Zn-free coupling agents," *Journal of Industrial and Engineering Chemistry*, vol. 66, no. 25, pp. 78–85, 2018.

[22] C. M. Flanigan, L. Beyer, D. Klekamp, D. Rohweder, B. Stuck, and E. R. Terrill, "Comparative study of silica, carbon black and novel fillers in tread compounds," *Rubber World*, vol. 245, no. 5, pp. 18–31, 2012.

[23] O. S. Kwon, D. Lee, S. P. Lee, Y. G. Kang, N. C. Kim, and S. H. Song, "Enhancing the mechanical and thermal properties of boron nitride nanoplatelets/elastomer nanocomposites by latex mixing," *RSC Advances*, vol. 6, no. 65, pp. 59970–59975, 2016.

[24] S. H. Song, J. M. Kim, K. H. Park et al., "High performance graphene embedded rubber composites," *RSC Advances*, vol. 5, no. 99, pp. 81707–81712, 2015.

[25] Q. Liu and K. Guo, "Features and Development of Tyre Cornering Characteristics," *Automobile Technology*, vol. 10, 1997.

[26] K. Guo, Y. Liu, and Y. Yang, "A developing study on experimental technique of tire with prospective application for vehicle performance," *Automobile Engineering*, vol. 1, 1990.

[27] Y. Ikeda, A. Katoh, J. Shimanuki, and S. Kohjiya, "Nanostructural observation of in situ silica in natural rubber matrix by three dimensional transmission electron microscopy," *Macromolecular Rapid Communications*, vol. 25, no. 12, pp. 1186–1190, 2004.

[28] N. Jouault, P. Vallat, F. Dalmas, S. Said, J. Jestin, and F. Boué, "Well-dispersed fractal aggregates as filler in polymer–silica nanocomposites: long-range effects in rheology," *Macromolecules*, vol. 42, no. 6, pp. 2031–2040, 2009.